European Journal of Chemistry 10 (3) (2019) 256-262

EurJChem
An International Open Access Journal

European Journal of Chemistry

ATLANTA PUBLISHING HOUSE

Synthesis, characterization and crystal structure of a novel tetranuclear Co(II) cubane cluster

Hong Chen [1,2], Jianchun Wu [1] and Mingguo Liu [2,*]

[1] Key Laboratory of Radiation Physics and Technology of Ministry of Education, Institute of Nuclear Science and Technology, Sichuan University, Chengdu 610064, P. R. China
chenhong3041@126.com (H.C.), 1624921422@qq.com (J.W.)
[2] Hubei Key Laboratory of Natural Products Research and Development, College of Biological and Pharmaceutical Sciences, China Three Gorges University, Yichang 443002, P. R. China
mgliu1966@163.com (M.L.)

* Corresponding author at: Hubei Key Laboratory of Natural Products Research and Development, College of Biological and Pharmaceutical Sciences, China Three Gorges University, Yichang 443002, P. R. China.
Tel: +86.717.6395580 Fax: +86.717.6395580 e-mail: mgliu1966@163.com (M. Liu).

RESEARCH ARTICLE

10.5155/eurjchem.10.3.256-262.1906

Received: 14 June 2019
Received in revised form: 07 July 2019
Accepted: 12 July 2019
Published online: 30 September 2019
Printed: 30 September 2019

KEYWORDS

Crystal structure
DFT calculations
2-Methylquinolin-8-ol
Transition-metal clusters
Tetranuclear Co(II) cubane
Hydrogen bonding interactions

ABSTRACT

A new tetranuclear Co(II) cubane cluster 1, $[Co_4(L1)_4(L2)_4]\cdot 4CH_3CH_2OH$ (HL1 = 2-Methylquinolin-8-ol, HL2 = t-Bu-COOH), has been synthesized and characterized by X-ray single crystal diffraction, FT-IR, TG/DSC, and elementary analysis. The data reveals that it has a very interesting structural motif consisting of a $[Co_4O_4]$ core in the form of a cube with the Co and O occupying opposite corners. In the crystal structure of complex 1, the molecules are linked by intramolecular C−H···O hydrogen bonding interactions and Van der Waals forces, forming a three-dimensional network structure. Crystal data for complex 1: $C_{60}H_{68}Co_4N_4O_{12}$, triclinic, space group P-1 (no. 2), with a = 12.0644(4), b = 12.0996(3), c = 20.2858(7) Å, α = 92.005(3)°, β = 92.182(3)°, γ = 97.943(3)°, Z = 2, V = 2928.25(16) Å^3, T = 293 K, μ(Mo$K\alpha$) = 1.178 mm^{-1}, D_{calc} = 1.444 g/cm^3, 16737 reflections measured ($3.00° \leq \theta \leq 28.53°$), 9010 unique ($R_{int}$ = 0.024, R_{sigma} = 0.0574) which were used in all calculations. The final R_1 was 0.039 ($I \geq 2\sigma(I)$) and wR_2 was 0.090 (all data).

Cite this: *Eur. J. Chem.* **2019**, *10(3)*, 256-262 **Journal website**: www.eurjchem.com

1. Introduction

In the past decade, much attention has been devoted to the study of polynuclear transition-metal clusters which is an essential part of coordination chemistry [1-5]. The coordination driven self-assembly has become one of the most convenient strategies for the bottom-up construction of functional molecular ensembles [6-9]. Moreover, it has become an interdisciplinary subject covering inorganic chemistry, organic chemistry, physical chemistry, biochemistry, supramolecular chemistry and materials chemistry [10-17]. Polynuclear transition-metal clusters have been fascinating scientists by their structural beauty and versatile functions, such that the design of metal clusters with potential applications such as magnetism [18-24], luminescence and bioactivity [25-28], and catalysis [29] is constantly being pursued. In addition, the search for key organic ligands is an important process to advance this investigation. 2-Methylquinolin-8-ol possessing one nitrogen atom and one terminal oxygen atom may provide the potential to construct unpredictable and interesting polymetallic clusters.

In this manuscript, we are reporting the synthesis and structural characterization of a novel tetranuclear Co(II) cubane cluster **1**, $[Co_4(L1)_4(L2)_4]\cdot 4CH_3CH_2OH$ (HL1 = 2-Methylquinolin-8-ol, HL2 = t-Bu-COOH). It has a P-1 space group exhibits a tetranuclear Co(II) cluster with a cubane topology in which the central Co(II) ion and oxygen atoms from chelating organic ligands (L1) occupy the alternate vertices of the cube. To the best of our knowledge, complex **1** was the first example of a coordination Co(II) cluster containing 2-methylquinolin-8-ol and pivalic acid group in the same cubane.

2. Experimental

2.1. Materials and apparatuses

2-Methylquinolin-8-ol and pivalic acid (t-Bu-COOH) were purchased from Alfa Aesar of 99.99% purity.

ISSN 2153-2249 (Print) / ISSN 2153-2257 (Online)
http://dx.doi.org/10.5155/eurjchem.10.3.256-262.1906

Table 1. Crystallographic data, details of data collection and structure refinement parameters for the complex **1**.

CCDC Number	1918368
Empirical formula	$C_{60}H_{68}Co_4N_4O_{12}$
Formula weight (g.mol^{-1})	1272.91
Crystal system	Triclinic
Space group	*P*-1
Morphology	Block
Size (mm)	0.38 × 0.26 × 0.15
a (Å)	12.0644(4)
b (Å)	12.0996(3)
c (Å)	20.2858(7)
α (°)	92.005(3)
β (°)	92.182(3)
γ (°)	97.943(3)
V (Å^3)	2928.25(16)
Z	2
T (K)	293
D_c (g.cm^{-3})	1.444
μ (mm^{-1})	1.178
F(000)	1320.0
Theta range for data collection (°)	$3.00 \leq \theta \leq 28.53$
h, k, l_{max}	16, 16, 27
Reflections collected / unique	16737/9010 [R_{int}=0.024]
Data/restraints/parameters	11317/0/737
R indices (all data)	R_1=0.0387, wR_2=0.0903
Largest diff. peak and hole (e Å^{-3})	0.43 and -0.41
S (GOF on F^2)	1.070

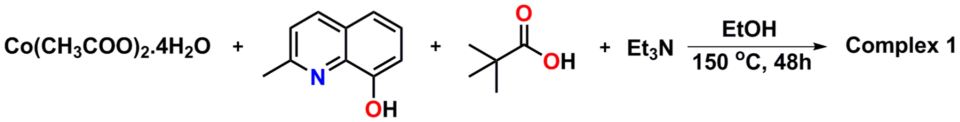

Scheme 1. Synthetic procedure for complex **1**.

Solvents were purified by established procedures [30]. All the other reagents were obtained from commercial sources with analytical grade and used without further purification. Infrared spectra were recorded by transmission through KBr pellets containing ca. 0.5% of the title compound using a PE Spectrum FT-IR spectrometer (400-4000 cm^{-1}). Elemental analysis (C, H, N) were taken on a Vario EL III elemental analysis instrument. Thermal gravimetry analyses (TGA) were carried out with a Universal V2.6 DTA system at a heating rate of 5 °C/min in a nitrogen atmosphere. Powder X-ray diffracttion intensities were measured at 293 K on a Rigaku D/Max-IIIA diffractometer (CuKα). The samples were prepared by crushing the single crystals and placed on a grooved aluminum plate, and the patterns were recorded from 5 to 45° at a rate of 5 °/min. Calculated diffraction patterns for the compounds were generated by Mercury 4.0 from the single-crystal data. Single-crystal X-ray diffraction data were collected on a SuperNova, Single source at offset, EOS diffractometer equipped with a graphite-monochromatic Mo*Kα* radiation (λ = 0.71073 Å). Crystal decay has not occurred during the data collection.

2.2. Synthesis and crystallization of complex 1

A mixture of $Co(CH_3COO)_2·4H_2O$ (124.5 mg, 0.5 mmol), HL1 (2-Methylquinolin-8-ol, 79.6 mg, 0.5 mmol), HL2 (Pivalic acid, 51.1 mg, 0.5 mmol), CH_3CH_2OH (16 mL), and $N(C_2H_5)_3$ (0.25 mL) was stirred at room temperature for one hour and then sealed in a 25 mL Teflon-lined stainless steel autoclave and heated to 150 °C for 2 days (Scheme 1). The autoclaves were then cooled to room temperature at a rate of 10 °C/h. Octahedral shaped purple crystals of complex **1** were collected, washed with CH_3CH_2OH, and then dried in air. $[Co_4(L1)_4(L2)_4]$ (**1**): Color: Purple. Yield: 33% (22.9 mg) based on $Co(CH_3COO)_2·4H_2O$). M.p.: 285-287 °C. Anal. calcd. for $C_{60}H_{68}Co_4N_4O_{12}$: C, 56.61; H, 5.38; N, 15.08. Found: C, 56.49; H, 5.22; N, 14.93 %. FT-IR (KBr, ν, cm^{-1}): 3417 (s), 2026 (w), 1619 (m), 1563 (m), 1503 (w), 1456 (w), 1403 (m), 1333 (w), 1169 (w), 1036 (w), 850 (w), 828 (w), 788 (w), 743 (w), 710 (w), 617 (w).

2.3. X-ray crystallography and refinement

Crystals suitable for X-ray diffraction were obtained by successfully selection of a single crystal from the obtained mixture. A purple single crystal of complex **1** with dimensions of 0.38 × 0.26 × 0.15 mm was selected and mounted on the top of a glass fiber. The data were collected by a SuperNova, Single source at offset, EOS diffractometer equipped with a graphite-monochromatic Mo*Kα* (λ = 0.71073 Å) radiation using a ω scan mode in the range of $3.0 \leq \theta \leq 28.53°$ ($-16 \leq h \leq 14$, $-15 \leq k \leq 16$, $-27 \leq l \leq 22$) at 293 K. A total of 16737 reflections were collected, of which 11317 were independent (R_{int} = 0.024) and 9010 were observed with $I > 2\sigma(I)$. All of the other crystal data, conditions of data collection and refinement are reported in Table 1.

Using Olex2 [31], the crystal structure of complex **1** was solved with the ShelXS structure solution program using Patterson Methods and refined with the ShelXL refinement package using Least Squares minimization [32]. The non-hydrogen atoms were refined isotropically. The F_o-F_c maps identified all the hydrogen atoms with electron densities higher than 2σ level and all hydrogen atoms were positioned geometrically (C-H = 0.93 Å for aromatic H, C-H = 0.96 Å for methyl H), and were included in the refinement in the riding model approximation, with $U_{iso}(H) = 1.2\ U_{eq}(C)$ for aromatic H atoms, and $U_{iso}(H) = 1.5\ U_{eq}(C)$ for methyl H atoms. The final R = 0.0387, wR = 0.0903 ($w = 1/[\sigma^2(Fo^2) + (0.0287P)^2 + 0.0551P]$, where $P = (Fo^2 + 2Fc^2)/3$). $(\Delta/\sigma)max < 0.001$, S = 1.070, $(\Delta\rho)max$ = 0.43 and $(\Delta\rho)min$ = −0.41 e/Å^3. The figures of the crystal structure for complex **1** were made using the DIAMOND program [33].

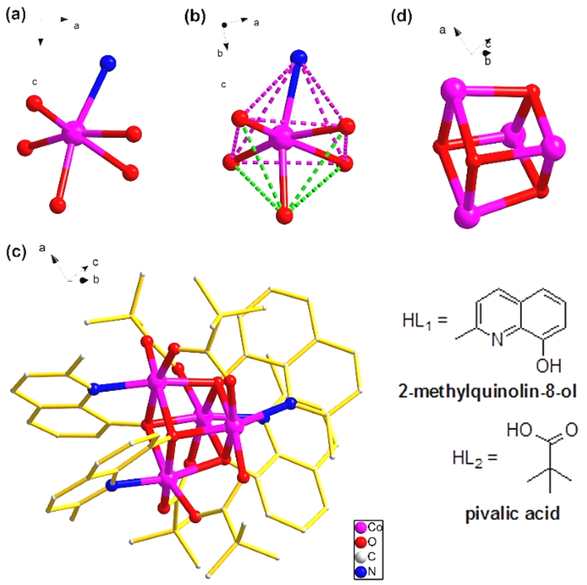

Figure 1. Structures of complex **1** (white, C; blue, N; red, O; and pink, Co). (a) Coordination mode and environment of Co(II) ions in complex **1**; (b) The distorted octahedral coordinated geometry of the Co(II) center, showing the Jahn-Teller effect of Co(II): $3d^7$-$(t_{2g})^5(e_g)^2$; (c) Crystal structure of the complex **1**, all of the hydrogen atoms have been omitted for clarity; (d) An example of the distorted $[Co_4O_4]$ cube structure in complex **1**.

2.4. Electronic structures calculations

The first-principles DFT calculation of complex **1** was done using the Vienna ab-initio simulation package (VASP 5.2.2) [34-36] performing a variational solution of the KohnSham equations in a plane-wave basis with energy cutoff of 300.0 eV. All atomic positions in complex **1** were fully relaxed without symmetry restrictions in a fixed unit cell parameters using a conjugate-gradient algorithm. For modeling of complex **1**, the unit cell parameters used were taken from the single crystal X-ray diffraction measurements. Electron exchange correlation interactions were treated using the generalized gradient approximation (GGA) as parameterized by Perdew, Burke and Ernzerhof (PBE) [37]. The electron ion interactions were described using the projector-augmented-wave (PAW) method [38]. The number of 9 valence electrons for each Co ($3d^74s^2$), 6 for O atom ($2s^22p^4$), 5 for N atom ($2s^22p^3$) and 4 for C atom ($2s^22p^2$) were treated explicitly and the remaining core electrons together with the nuclei were described by PAW pseudopotentials.

To describe correctly the strong Coulomb repulsion (U) between the localized d electrons of Co, the DFT + U approach, adding a Hubbard-like term to the effective potential was applied in all calculations as implemented in VASP package. In the present work, the approach described by Dudarev *et al.* [39] was applied, where an effective Hubbard parameter $U_{eff} = U\text{-}J$ enters the Hamiltonian, with U and J being the Coulomb (of 4 eV) and exchange interaction parameter (of 1 eV), respectively.

3. Result and discussion

3.1. Description of crystal structure of complex 1

Complex **1** has a very interesting structural motif consisting of a $[Co_4O_4]$ core in the form of a cube with four cobalt atoms and four oxygen atoms occupying opposite corners (Figure 1(c) and 1(d)). In other words, one can consider it as the interpenetration of two tetrahedral Co and O sublattices, similar to what was observed in the previously published $[Co_4L_4(MeOH)_4]$ and $[Ni_4L_4(MeOH)_4]$ compounds [22,40-42]. The $[Co_4O_4]$ cube is distorted because of the strong Jahn-Teller effect of divalent Co($3d^7$) (Figure 1(a) and 1(b)). The central Co atom has a distorted octahedral coordination environment with one N atom and five O atoms. Each metal adopts a distorted-octahedral geometry consisting of chelating organic ligands (HL1 = 2-Methylquinolin-8-ol) where the nitrogen is singly bonded but the phenoxy oxygen atom acts as a triple bridge at the corner of the cube (Table 2 and Figure 1(c)). The remaining two sites of the $[Co_4O_4]$ cube are then taken by the other organic ligands (HL2 = t-Bu-COOH). The metal centers are equivalent in the highly symmetric structure of the complex **1**. Meanwhile, the sites of the two kind of chelating organic ligands are also totally equivalent.

The $[Co_4O_4]$ core is a fairly stable geometry with Co-O and Co-N distances lying within observed ranges of coordination compounds and the angles vary in a wider range. The distances of Co(1)-O(1) and Co(1)-N(3) in complex **1** are 2.1329(18) and 2.1373(22) Å, respectively (Table 2). The Co···Co distances (3.090-3.353 Å) are normal to those bridged by two oxygen atoms [18,36]. And the Co-O-Co angles can vary in the range of 91.57(6)-103.78(7)°. In the crystal structure the chelating organic ligands (L1) are paired almost face to face on opposite side of the $[Co_4O_4]$ core. This leaves the carbonyl group (L2) to lie in a plane perpendicular to that of the $[Co_4O_4]$ cube. Several supramolecular interactions, including intramolecular C(2)-H(2)···O(5), C(12)-H(12)···O(8), C(32)-H(32)···O(12), C(10)-H(10C)···O(11) and C(20)-H(20A)···O(10) hydrogen bonding interactions are present within the structures (Figure 2 and Table 3). This leads to distinct bond lengths and angles for the three different types of cube faces, resulting in shorter Co···Co distances and deformation of the cubane core away from ideal cubic symmetry. The bidentate organic ligands (L1) are paired and located on the opposite face of the cube, and the pairs are pseudo-orthogonal. This choice of geometry favors an efficient packing and allows for supramolecular interaction between molecules (Figure 3). The shortest distance between the centers of the $[Co_4O_4]$ cubes is 12.06 Å (Figure 3 and 4). Powder diffraction patterns of as-synthesized sample and single-crystal simulation for complex **1** are given in Figure 5.

Table 2. Selected bond lengths (Å) and bond angles (°) of the complex **1**.

Atom-Atom	Bond distance	Atom-Atom	Bond distance	Atom-Atom-Atom	Angle
Co(1)-O(7)	2.0074(17)	Co(3)-O(11)	1.9922(18)	O(7)-Co(1)-O(3)	166.79(7)
Co(1)-O(3)	2.0810(16)	Co(3)-O(8)	2.0457(17)	O(7)-Co(1)-O(5)	105.69(7)
Co(1)-O(5)	2.0873(18)	Co(3)-O(1)	2.0798(17)	O(3)-Co(1)-O(5)	84.86(7)
Co(1)-O(1)	2.1329(17)	Co(3)-O(2)	2.1440(17)	O(7)-Co(1)-O(1)	86.31(7)
Co(1)-N(3)	2.137(2)	Co(3)-N(1)	2.147(2)	O(3)-Co(1)-O(1)	86.04(6)
Co(1)-O(2)	2.1775(17)	Co(3)-O(4)	2.1773(17)	O(5)-Co(1)-O(1)	88.55(7)
Co(2)-O(6)	1.9985(17)	Co(4)-O(10)	2.0037(18)	O(7)-Co(1)-N(3)	107.66(8)
Co(2)-O(4)	2.0722(17)	Co(4)-O(12)	2.0800(17)	O(3)-Co(1)-N(3)	79.73(7)
Co(2)-O(9)	2.0813(17)	Co(4)-O(2)	2.0828(17)	O(5)-Co(1)-N(3)	90.12(7)
Co(2)-O(3)	2.1425(17)	Co(4)-O(4)	2.1194(18)	O(1)-Co(1)-N(3)	165.77(7)
Co(2)-N(4)	2.155(2)	Co(4)-N(2)	2.138(2)	O(6)-Co(2)-O(4)	165.48(7)
Co(2)-O(1)	2.1787(16)	Co(4)-O(3)	2.1891(16)	O(6)-Co(2)-O(9)	106.39(7)
O(1)-C(1)	1.354(3)	O(2)-C(11)	1.345(3)	O(11)-Co(3)-O(8)	104.53(8)
O(3)-C(21)	1.357(3)	O(4)-C(31)	1.350(3)	Co(4)-O(2)-Co(1)	103.78(7)
C(1)-C(2)	1.369(4)	C(1)-C(9)	1.435(3)	Co(2)-O(3)-Co(4)	91.57(6)
C(8)-N(1)	1.334(3)	C(9)-N(1)	1.372(3)	Co(4)-O(4)-Co(3)	92.45(7)
Co(1)···Co(2)	3.117(5)	Co(2)···Co(3)	3.328(5)	Co(3)-O(1)-Co(1)	94.36(7)
Co(1)···Co(3)	3.090(5)	Co(2)···Co(4)	3.105(5)	Co(3)-O(1)-Co(2)	102.79(7)
Co(1)···Co(4)	3.353(5)	Co(3)···Co(4)	3.103(6)	Co(1)-O(1)-Co(2)	92.59(6)

Table 3. Intramolecular hydrogen bond lengths (Å) and bond angles (°) of the complex **1**.

D-H···A	d(D-H)	d(H···A)	d(D···A)	∠D-H···A
C(2)-H(2)···O(5)	0.93	2.55	3.2878	136
C(10)-H(10C)···O(11)	0.96	2.52	3.1982	128
C(12)-H(12)···O(8)	0.93	2.54	3.2775	136
C(20)-H(20A)···O(10)	0.96	2.54	3.1701	123
C(29)-H(29A)···O(7)	0.96	2.31	3.2383	161
C(32)-H(32)···O(12)	0.93	2.54	3.2599	134
C(40)-H(40C)···O(6)	0.96	2.36	3.2842	161
C(45)-H(45C)···O(6)	0.96	2.48	2.8342	102
C(48)-H(48B)···O(8)	0.96	2.48	2.8312	102

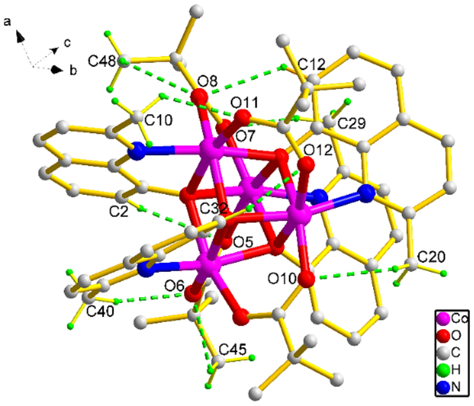

Figure 2. Emphasis of the cubane-like $[Co_4O_4]$ fragment and C-H···O hydrogen bonding interactions in complex **1**. Most hydrogen atoms have been omitted for clarity. The green dashed lines demonstrate the hydrogen bonding interactions.

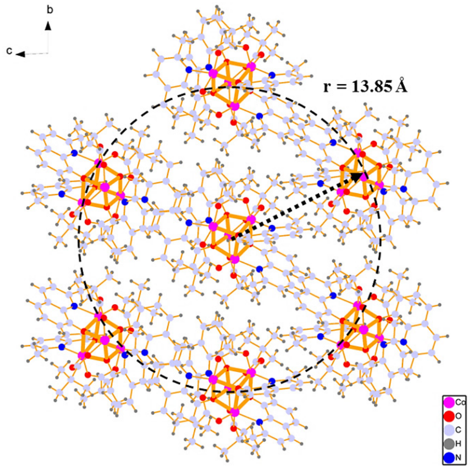

Figure 3. Packing diagram of the tetranuclear Co(II) cubane clusters (triclinic system) within the crystallographic *bc* plane (white, C; gray, H; blue, N; red, O; and pink, Co). Intramolecular C-H···O hydrogen bonding interactions, as well as Van der Waals forces, help to stabilize the crystal structures and form a three-dimensional network.

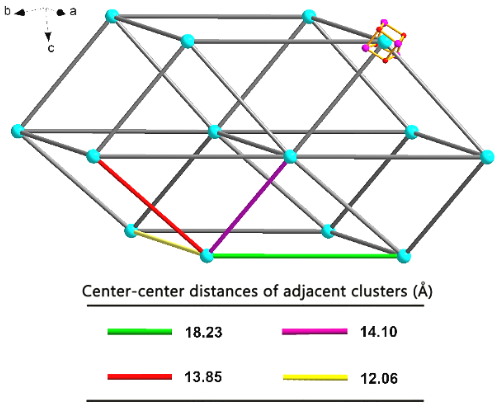

Figure 4. Illustrative representation of the links between [Co_4O_4] cube centers. The cyan balls were used to stand for the centers of [Co_4O_4] cubes. All of the other atoms have been omitted for clarity.

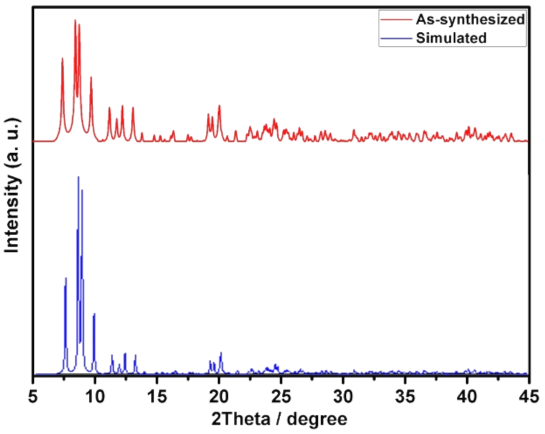

Figure 5. Powder diffraction patterns of as-synthesized sample and single-crystal simulation for complex **1**.

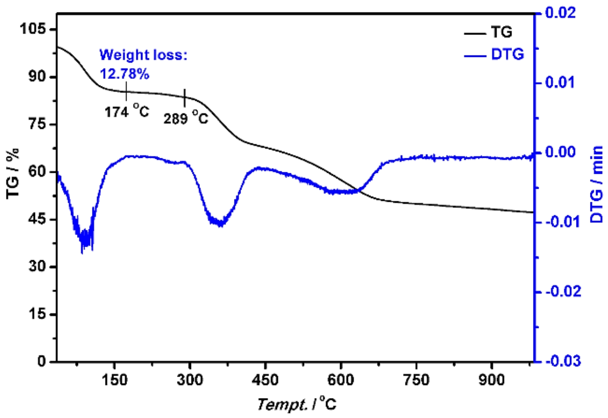

Figure 6. Thermogravimetry of the complex **1** at a heating rate of 5 °C/min under N_2 atmosphere.

3.2. Thermal behaviors of complex 1

In order to characterize the thermal stability of complex **1**, its thermal decomposition behavior was investigated as shown in Figure 6. In the TG/DSC analysis, there exists a weight loss of 12.78% occurring below 200 °C, which correspond to the continuous loss of four guest EtOH molecules and can be compared with the calculated value of 12.65%. The second stage weight loss can be detected from 289 to 450 °C attributed to the departure of $L2^-$ ligands. Above 460 °C, the compound begins to lose $L1^-$ ligands and then the whole framework starts to decompose.

3.3. Electronic density of state (DOS)

In order to better understanding the electronic properties of complex **1**, its electronic properties are investigated through the electronic density of states (DOS) and partial density of states (PDOS) spectra. All of these spectra for the complex **1** are presented in Figure 7. Moreover, the PDOS spectra of the atoms which are interacted in the considered configurations (Co, O, N atoms) are presented in Figure 7(b-d) for deeper analysis. Band structure calculations for complex **1** predicted the Fermi energy convergence tolerance at 0.2721×10^{-13} eV and Fermi energy for spin-degenerate system at 1.43574 eV, which were consistent with the magnitude and order of other experimental results.

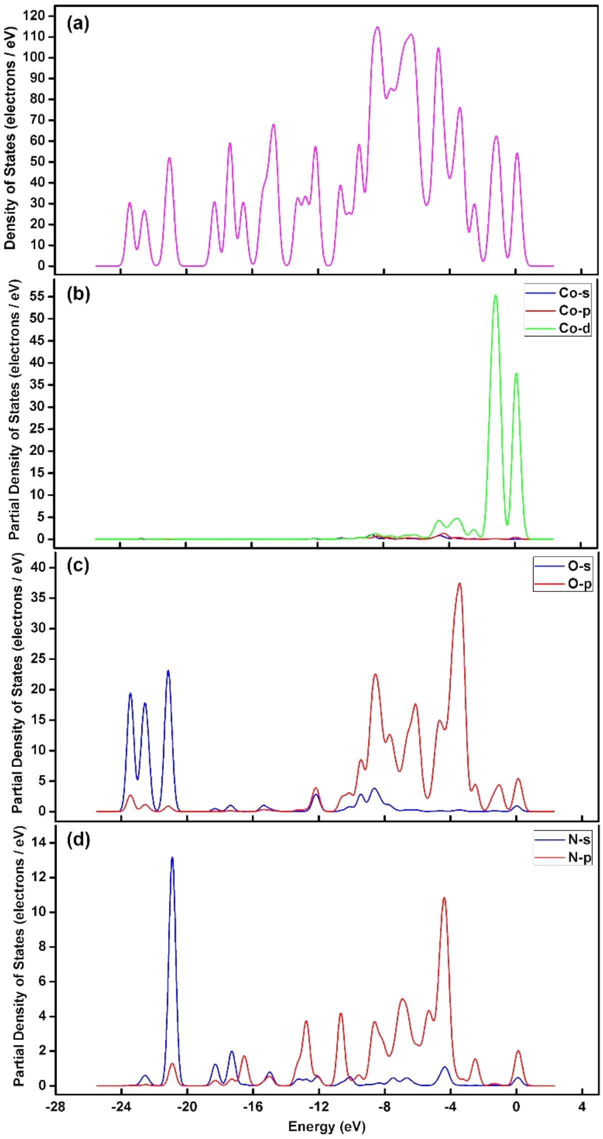

Figure 7. (a) Density of states (DOS) spectra and (b-d) partial density of states (PDOS) spectra of complex **1** obtained by DFT calculation. The blue, red and green lines represent s, p and d orbitals, respectively. The Fermi level sets to zero.

The calculated DOS spectra (Figure 7(a)) of complex **1** exhibit a strong peak at nearly 52 eV near the Fermi level, which belongs to the 3d orbitals of the Co atom (Figure 7(b)), demonstrates its semiconductor character.

4. Conclusions

The reported work describes the synthesis, single crystal X-ray diffraction analysis and electronic structures calculations of a novel tetranuclear Co(II) cubane cluster **1**, $[Co_4(L1)_4(L2)_4]\cdot 4CH_3CH_2OH$. The study of X-ray single crystal diffraction shows that complex **1** has a very interesting structural motif consisting of a $[Co_4O_4]$ core in the form of a cube with the Co and O occupying opposite corners. It crystallized in triclinic crystal system, *P*-1 (no. 2) space group. In the single crystal of complex **1**, the strong classical and non-classical intermolecular hydrogen bonds are not found. In addition, the supramolecular aggregation of complex **1** is stabilized *via* intramolecular C-H···O hydrogen bonding interactions as well as Van der Waals forces, forming a three-dimensional network structure.

Acknowledgements

The authors acknowledge the Analytical & Testing Center of China Three Gorges University for the X-ray single crystal diffractometer work. The authors are also grateful to Dr. Daichuan Ma for help with the single crystal measurements. Meanwhile, the authors would like to thank the Institute of Nuclear Science and Technology, Sichuan University for the first-principles DFT calculation of complex **1** by using the Vienna ab-initio simulation package (VASP 5.2.2). The authors also give their sincerely thanks to Dr. Yu Zou and Dr. Huan Wang for valuable discussions and for the help on the work of electronic structures calculations.

Supporting information S

CCDC 1918368 contains the supplementary crystallographic data for this paper. These data can be obtained free of charge via https://www.ccdc.cam.ac.uk/structures/, or by e-mailing data_request@ccdc.cam.ac.uk, or by contacting The Cambridge Crystallographic Data Centre, 12 Union Road, Cambridge CB2 1EZ, UK; fax: +44(0)1223-336033.

Disclosure statement

Conflict of interests: The authors declare that they have no conflict of interest.
Author contributions: All authors contributed equally to this work.
Ethical approval: All ethical guidelines have been adhered.
Sample availability: Samples of the compounds are available from the author.

ORCID

Hong Chen
http://orcid.org/0000-0002-8415-7333
Jianchun Wu
http://orcid.org/0000-0002-8227-4640
Mingguo Liu
http://orcid.org/0000-0003-2686-3034

References

[1]. Fujita, D.; Ueda, Y.; Sato, S.; Mizuno, N.; Kumasaka, T.; Fujita, M. *Nature* **2016**, *540*, 563-566.
[2]. Brown, C. J.; Toste, F. D.; Bergman, R. G.; Raymond, K. N. *Chem. Rev.* **2015**, *115*, 3012-3035.
[3]. McConnell, A. J.; Wood, C. S.; Neelakandan, P. P.; Nitschke, J. R. *Chem. Rev*. **2015**, *115*, 7729-7793.
[4]. Saha, M. L.; Yan, X.; Stang, P. J. *Acc. Chem. Res.* **2016**, *49*, 2527-2539.
[5]. Ballester, P.; Fujita, M.; Rebek, Jr. J. *Chem. Soc. Rev.* **2015**, *44*, 392-393.
[6]. Cook, T. R.; Stang, P. J. *Chem. Rev.* **2015**, *115*, 7001-7045.
[7]. Smulders, M. M. J.; Riddell, I. A.; Browne, C.; Nitschke, J. R. *Chem. Soc. Rev*. **2013**, *42*, 1728-1754.
[8]. Han, M.; Engelhard, D. M.; Clever, G. H. *Chem. Soc. Rev.* **2014**, *43*, 1848-1860.
[9]. Saalfrank, R. W.; Maid, H.; Scheurer, A. *Angew. Chem. Int. Ed.* **2008**, *47*, 8794-8824.
[10]. Yoshizawa, M.; Klosterman, J. K.; Fujita, M. *Angew. Chem. Int. Ed.* **2009**, *48*, 3418-3438.
[11]. Breiner, B.; Clegg, J. K.; Nitschke, J. R. *Chem. Sci.* **2011**, *2*, 51-56.
[12]. Galan, A.; Ballester, P. *Chem. Soc. Rev.* **2016**, *45*, 1720-1737.
[13]. Koblenz, T. S.; Wassenaar, J.; Reek J. N. H. *Chem. Soc. Rev.* **2008**, *37*, 247-262.
[14]. Georgieva, I.; Trendafilova, N.; Dodoff, N.; Kovacheva. D. *Spectrochim. Acta A* **2017**, *176*, 58-66.
[15]. Song, J.; Duan, B. F.; Lu, J. F.; Wu, R.; Du. Q. C. *J. Mol. Struct.* **2019**, *1195*, 252-258.
[16]. Akhtar, M.; Alharthi, A. I.; Alotaibi, M. A.; Trendafilova, N. *Polyhedron* **2017**, *122*, 105-115.
[17]. Chen, H.; Liu, M. G. *J. Mol. Struct.* **2019**, *1180*, 31-40.
[18]. Jeon, I. R.; Clérac, R. *Dalton Trans.* **2012**, *41*, 9565-9686.
[19]. Sato, Y.; Ohkoshi, S.; Arai, K.; Tozawa, M.; Hashimoto, K. *J. Am. Chem. Soc.* **2003**, *125*, 14590-14595.
[20]. Liu, C. M.; Zhang, D. Q.; Zhu, D. B. *Chem. Commun.* **2008**, 368-370.
[21]. Hao, Z. M.; Zhang, X. M. *Dalton Trans.* **2011**, *40*, 2092-2098.
[22]. Das, A.; Klinke, F. J.; Demeshko, S.; Meyer, S.; Dechert, S.; Meyer, F. *Inorg. Chem.* **2012**, *51*, 8141-8149.
[23]. Murrie, M.; Teat, S. J.; Stoeckli-Evans, H.; Gudel, H. U. *Angew. Chem., Int. Ed.* **2003**, *42*, 4653-4656.
[24]. Song, Y. M.; Luo, F.; Luo, M. B.; Liao, Z. W.; Sun, G. M.; Tian, X. Z.; Zhu, Y.; Yuan, Z. J.; Liu, S. J.; Xu, W. Y.; Feng, X. F. *Chem. Commun.* **2012**, *48*, 1006-1008.
[25]. Zeng, M. H.; Yin, Z.; Liu, Z. H.; Xu, H. B.; Feng, Y. C.; Hu, Y. Q.; Chang, L. X.; Zhang, Y. X.; Huang, J.; Kurmoo, M. *Angew. Chem., Int. Ed.* **2016**, *55*, 11407-11411.
[26]. Shi, X. C.; Chen, Z. Y.; Wang, Y. J.; Guo, Z. J.; Wang, X. Y. *Dalton Trans.* **2018**, *47*, 5049-5054.
[27]. Hannon, M. J. *Chem. Soc. Rev.* **2007**, *36*, 280-295.
[28]. Hannon, M. J. *Pure Appl. Chem.* **2007**, *79*, 2243-2261.
[29]. Passard, G.; Ullman, A. M.; Brodsky, C. N.; Nocera, D. G. *J. Am. Chem. Soc.* **2016**, *138*, 2925-2928.
[30]. Becker, H. G. O.; Berger, W.; Domschke, G.; Fanghanel, E.; Faust, J.; Fischer, M.; Gentz, F.; Gewald, K.; Gluch, R.; Mayer, R.; Müller, K.; Pavel, D.; Schmidt, H.; Schollberg, K.; Schwetlick, K.; Seiler, E.; Zeppenfeld, G. *Organikum*, 19th ed.; Johann Ambrosius Barth Verlag GmbH: Leipzig, Berlin, Heidelberg, 1993.
[31]. Dolomanov, O. V.; Bourhis, L. J.; Gildea, R. J.; Howard, J. A. K.; Puschmann, H. *J. Appl. Cryst.* **2009**, *42*, 339-341.
[32]. Sheldrick, G. M. *Acta Cryst. A* **2008**, *64*, 112-122.
[33]. K. Brandenburg, DIAMOND Version 3.0, Crystal Impact GbR, Bonn, Germany, 2014.
[34]. Kresse, G.; Hafner, J. *Phys. Rev. B* **1993**, *47*, 558-561.
[35]. Kresse, G.; Hafner, J. *Phys. Rev. B* **1994**, *49*, 14251-14269.
[36]. Kresse, G.; Furthmüller, J. *Phys. Rev. B* **1996**, *54*, 11169-11186.
[37]. Perdew, J. P.; Burke, K.; Ernzerhof, M. *Phys. Rev. Lett.* **1996**, *77*, 3865-3868.
[38]. Kresse, G.; Joubert, D. *Phys. Rev. B* **1999**, *59*, 1758-1775.
[39]. Dudarev, S. L.; Botton, G. A.; Savrasov, S. Y.; Humphreys, C. J.; Sutton, A. P. *Phys. Rev. B* **1998**, *57*, 1505-1509.
[40]. Klinke, F. J.; Das, A.; Demeshko, S.; Dechert, S.; Meyer, F. *Inorg. Chem.* **2014**, *53*, 2976-2982.
[41]. Ma, X. F.; Wang, Z.; Chen, X. L.; Kurmoo, M.; Zeng, M. H. *Inorg. Chem.* **2017**, *56*, 15178-15186.
[42]. Chen, X. L.; Xu, H. B.; Shi, X. X.; Zhang, Y. X.; Yang, T.; Kurmoo, M.; Zeng, M. H. *Inorg. Chem.* **2017**, *56*, 14069-14076.